ELSEVIER

Thermochimica Acta 345 (2000) 145–156

thermochimica acta

www.elsevier.com/locate/tca

Infrared emission spectroscopic study of the dehydroxylation of some hectorites

J.T. Kloprogge*, R.L. Frost, L. Hickey

Centre for Instrumental and Developmental Chemistry, Queensland University of Technology, 2 George Street, GPO Box 2434, Brisbane Qld 4001, Australia

Received 24 March 1999; accepted 24 September 1999

Abstract

The structural changes of three hectorites during dehydroxylation have been studied using Infrared emission spectroscopy of the hydroxyl stretching and bending regions. The hydroxyl stretching region is characterised by two hydroxyl stretching modes around 3647 and 3672 cm^{-1}. These bands decrease in intensity upon dehydroxylation up to 750°C but do not completely disappear. Above 250°C a new band attributed to silanol groups becomes visible around 3741 cm^{-1} in all samples due to transfer of the hydroxyls from the octahedral layer to the siloxane layer before they are lost. The presence of two different hydroxyl groups is also reflected in the hydroxyl deformation modes around 657 and 695 cm^{-1}. These bands show a decrease in intensity upon heating and dehydroxylation of the clay structure. A new broad band becomes visible at high temperature, which is ascribed to the formation of pyroxene-like ($MgSiO_3$) units. The infrared emission spectra do not give any evidence of what happens to the lithium and other interlayer alkalies during the dehydroxylation but it is inferred that the lithium is incorporated in an amorphous silica phase.

Keywords: Dehydroxylation; Hectorite; Infrared absorption spectroscopy; Infrared emission spectroscopy; Smectite; Thermal transformation

1. Introduction

Smectites are 2:1 phyllosilicates or layer silicates, which have a layered structure in which two-dimensional oxo-anions are separated by layers of hydrated cations. The oxygen atoms define upper and lower sheets enclosing tetrahedral sites and a central sheet having the brucite or gibbsite structure enclosing octahedral sites. Hectorite is a trioctahedral smectite, which in theory means that all of the octahedral sites are filled with divalent metal cations. This in contrast to the dioctahedral smectites in which only 2/3 of the sites are occupied by a trivalent metal cation and the remaining sites are vacant [1]. The theoretical composition of a hectorite can be visualised as $M^{n+}_{x/n}(Mg_{6-x}Li_x)Si_8O_{20}(OH,F)_4{\cdot}nH_2O$ with x generally around 0.7 [2,3]. Natural hectorite and the comparable clay mineral stevensite generally contain only minor amounts of trivalent cations. Hectorite is a rather unusual smectite as it contains essentially F and Li, where the substitution of Li for Mg creates the negative charge on the layers [1,4]. The tetrahedral sheet contains mainly Si and does not contribute to the layer charge. Stevensite is very closely related to hectorite but the negative charge on the layers is approximately half of that of hectorite and other

* Corresponding author. Tel.: +31-7-38641220; fax: +61-7-3864-1804.
E-mail address: t.kloprogge@qut.edu.au (J.T. Kloprogge).

0040-6031/00/$ – see front matter
PII: S0040-6031(99)00359-7

smectites and is caused by a small deficiency of octahedral cations creating vacant sites in the octahedral sheet. Often Li substitution and vacancies are present together in the same octahedral sheet.

The hydroxyl-stretching region of hectorites is characterised by possibly four hydroxyl bands associated with the Mg and Li occupying two of the three possible octahedral sites. In general the Mg_3OH bands are shifted by about 20 cm^{-1}, compared to e.g. talc and saponite, to values around 3700 cm^{-1} [5,6]. Komadel et al. [7] reported only a single band at 3675 cm^{-1} for hectorite from Hector, CA. The corresponding vibration band can be found around 654–657 cm^{-1}, compared to 669 cm^{-1} for talc [6–9]. Farmer [10] also reported only one band around 3678 cm^{-1} for hectorite SHCa-1. Torii and Iwasaki [11] found a single band around 3680 cm^{-1} for synthetic hectorite. Li in hectorite is probably associated with the F substituting the hydroxyl group, but the exact effect on the hydroxyl stretching frequencies is not completely clear. Calvet and Prost [12] for example have observed a band at 3640 cm^{-1} in montmorillonite. Gadsden [8] reported a doublet around 3670–3610 cm^{-1} without assignment. Van der Marel and Beutelspacher [13] observed two bands at 3680 and 3623 cm^{-1}. In addition a broad band was observed around 3450–3400 cm^{-1} with a shoulder around 3250–3200 cm^{-1}. A similar band around 3430 cm^{-1} has been observed for synthetic beidellite and saponite and has been ascribed to hydroxyl groups involved in the water–water hydrogen-bond [14,15]. For both beidellite and saponite a second type of water band has been reported around 3250 cm^{-1}, which was not reported by Gadsden [8]. Farmer [6] assigned this band as an overtone of the water-bending mode around 1630 cm^{-1}. These very broad water bands observed for smectites tend to mask the metal–OH stretching modes. This is especially true for hectorite [13].

The hectorite spectra show a marked broadening and some displacements of the bands in the low frequency region compared to talc, from which the structure can be derived by substitution of Li for Mg. Almost no effect is observed for the Si–O vibrations around 1000 and 450 cm^{-1} as they are not influenced by the substitution. However, important differences can be observed between talc, saponite and hectorite in the region between 900 and 500 cm^{-1} [6]. Komadel et al. and Madejova et al. reported the main Si–O in-plane stretching mode around 1012–1015 cm^{-1} and the out-of-plane mode around 1070 cm^{-1}, accompanied by the out-of-plane and in-plane bending modes around 701–703 and 467–469 cm^{-1} [7,9]. Carbonate bands due to the presence of calcite in their sample were observed at 1432 and 874 cm^{-1}. A Mg–O band was observed at 522 cm^{-1}. These band positions are in good agreement with the spectrum reported by van der Marel and Beutelspacher, although they also reported two extra bands at 449 and 427 cm^{-1} for hectorite from the same locality [13]. Torii and Iwasaki reported significantly shifted (up to 20 cm^{-1}) band positions at 995, 700, 660, 540, 455 and 390 cm^{-1} for synthetic hectorite in comparison to the studies discussed above [11]. However, they claim that the synthetic hectorite spectrum is similar to that of a natural stevensite from the Obori Mine, Yamagata, Prefecture in Japan previously reported by Shimoda [16].

The dehydroxylation behaviour of hectorite has never been studied in detail by in situ spectroscopic methods. The technique of measurement of discrete vibrational frequencies emitted by thermally excited molecules, known as Fourier transform infrared emission spectroscopy (FTIR ES, or shortly IES) [17–19] has not been widely used for the study of mineral and especially clay structures although the interest in this technique is growing (see for example [15,20–29]). The major advantages of IES are that the samples are measured in situ at elevated temperatures and IES requires no sample treatment other than making the sample of submicron particle size. Further the technique removes the difficulties of heating the sample to dehydroxylation temperatures and subsequent quenching prior to the measurement, as IES measures the dehydroxylation process as it is actually taking place. In this paper we report the results of an extended IES and FTIR study of the dehydroxylation of some natural hectorites.

2. Materials and methods

2.1. Hectorite

The first hectorite was supplied by the Clay Minerals Society as Source clay SHCa-1. This clay originates from the Pliocene Red Mountain Andesite formation, County of San Bernardino, CA [30]. The

Table 1
Chemical analyses (%) of the standard hectorite samples [4,30]

	SHCa-1	API No. 34
SiO_2	34.7	55.86
Al_2O_3	0.69	0.13
TiO_2	0.038	–
Fe_2O_3	0.02	0.03
FeO	0.25	
MnO	0.008	–
MgO	15.3	25.03
CaO	23.4	Trace
Na_2O	1.26	2.68
K_2O	0.13	0.10
Li_2O	2.18	1.05
F	2.60	5.96
H_2O	20.6	9.90
Total	101.18	100.74

sample contains quartz and calcite as impurities according to the specifications. The second hectorite was supplied as a standard clay by Ward (API No. 34) and originates from the type locality Hector, CA. This sample contains some calcite as an impurity. The chemical compositions of the standard clays are given in Table 1. The third sample named hectorite E was collected in Western Australia and supplied by CSIRO Adelaide (Phil Slade). Hectorite E was Ca-saturated before characterisation.

2.2. X-ray diffraction

The X-ray diffraction (XRD) analyses were carried out on a Philips wide angle PW 1050/25 vertical goniometer equipped with a graphite diffracted beam monochromator. The *d*-values and intensity measurements were improved by application of an in-house developed computer aided divergence slit system enabling constant sampling area irradiation (20 mm long) at any angle of incidence. The goniometer radius was enlarged to 204 mm. The radiation applied was $Cu_{K\alpha}$ from a long fine focus Cu tube operating at 35 kV and 40 mA. The samples were measured at 50% relative humidity in stepscan mode with steps of 0.02° 2θ and a counting time of 2 s.

2.3. FTIR spectroscopy

All samples were oven dried to remove any adsorbed water. Each sample (1 mg) was combined with oven dried spectroscopic grade KBr (±250 mg) and pressed into a disc using 8 tonnes of pressure for 5 min under vacuum. The spectrum of each sample was recorded in triplicate by accumulating 64 scans at 4 cm^{-1} resolution between 400 and 4000 cm^{-1} using the Perkin-Elmer 1600 series Fourier transform infrared spectrometer equipped with a LITA detector.

2.4. Infrared emission spectroscopy

FTIR ES was carried out on a Digilab FTS-60A spectrometer, which was modified by replacing the IR source with an emission cell. A description of the cell and principles of the emission experiment have been published elsewhere [17–19]. Approximately 0.2 mg of the clay sample was spread as a thin layer on a 6 mm diameter platinum surface and held in an inert atmosphere within a nitrogen-purged cell during heating. The infrared emission cell consists of a modified atomic absorption graphite rod furnace, which is driven by a thyristor-controlled AC power supply capable of delivering up to 150 amps at 12 V. A platinum disk acts as a hot plate to heat the sample and is placed on the graphite rod. An insulated 125 μm type R thermocouple was embedded inside the platinum plate in such a way that the thermocouple junction was <0.2 mm below the surface of the platinum. Temperature control of ±2°C at the operating temperature of the sample was achieved by using an Eurotherm Model 808 proportional temperature controller, coupled to the thermocouple.

The design of the IES facility is based on an off axis paraboloidal mirror with a focal length of 25 mm mounted above the heater captures the infrared radiation and directs the radiation into the spectrometer. The assembly of the heating block, and platinum hot plate is located such that the surface of the platinum is slightly above the focal point of the off axis paraboloidal mirror. By this means the geometry is such that approximately 3 mm diameter area is sampled by the spectrometer. The spectrometer was modified by the removal of the source assembly and mounting a gold-coated mirror, which was drilled through the centre to allow the passage of the laser beam. The mirror was mounted at 45°, which enables the IR radiation to be directed into the FTIR spectrometer.

In the normal course of events, three sets of spectra are obtained: firstly the black body radiation over the

temperature range selected at the various temperatures; secondly the platinum plate radiation is obtained at the same temperatures and; thirdly the spectra from the platinum plate covered with the sample. Normally only one set of black body and platinum radiation is required. The emittance spectrum at a particular temperature was calculated by subtraction of the single beam spectrum of the platinum backplate from that of the platinum + sample, and the result ratioed to the single beam spectrum of an approximate blackbody (graphite). This spectral manipulation is carried out after all the spectral data have been collected.

The emission spectra were collected at intervals of 50°C over the range 200–750°C. The time between scans (while the temperature was raised to the next hold point) was approximately 100 s. It was considered that this was sufficient time for the heating block and the powdered sample to reach temperature equilibrium. The spectra were acquired by coaddition of 64 scans for the whole temperature range (approximate scanning time 45 s), with a nominal resolution of 4 cm^{-1}. Good quality spectra can be obtained provided the sample thickness is not too large. If too a large sample is used then the spectra become difficult to interpret as a result of reabsorption.

Data interpretation and manipulation for both FTIR and IES was carried out using the Spectracalc software package GRAMS (Galactic Industries, NH, USA) and Microsoft Excel. The band-positions and intensities of the bands were determined by band component analysis using the Jandel 'Peakfit' software package.

3. Results and discussion

The powder XRD patterns of the various hectorite samples are shown in Fig. 1. Hectorite SHCa-1 contains as expected quartz and calcite as impurities, but also a minor amount of dolomite. Careful washing with diluted acetic acid removed all the carbonates, while sedimentation removed the quartz. Care has been taken not to affect the hectorite crystals by the acid treatment causing an attack of protons on the octahedral Li sites [7,31]. Also the hectorite from Hector (Ward's) contains some calcite and dolomite, whereas hectorite E from Australia contains a significant amount of dolomite in addition to a relatively small amount of calcite. The presence of dolomite is not really surprising as hectorite and stevensite are generally formed in Mg, Ca and carbonate rich environments [1,32].

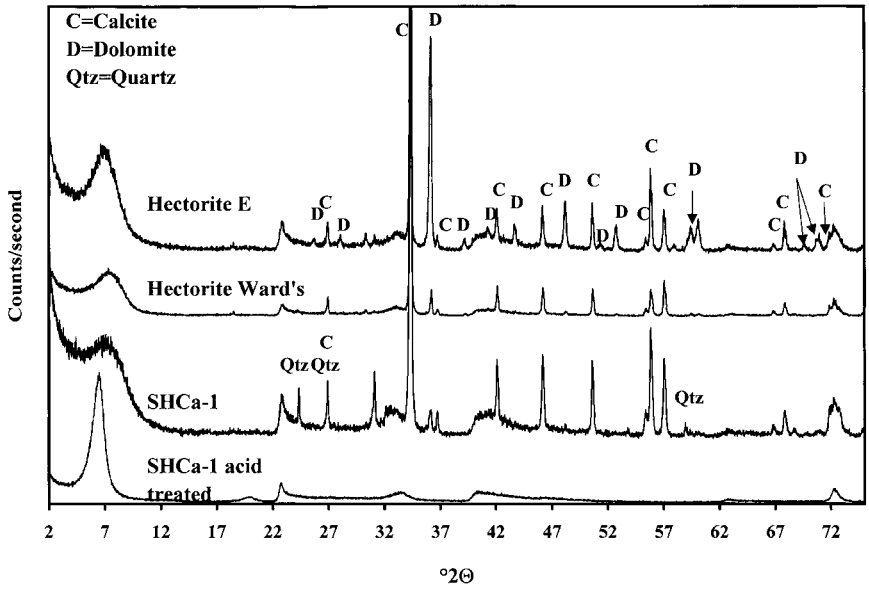

Fig. 1. XRD patterns of hectorite SHCa-1, acetic acid treated SHCa-1, Ward's hectorite from Hector (CA) and hectorite from Western Australia.

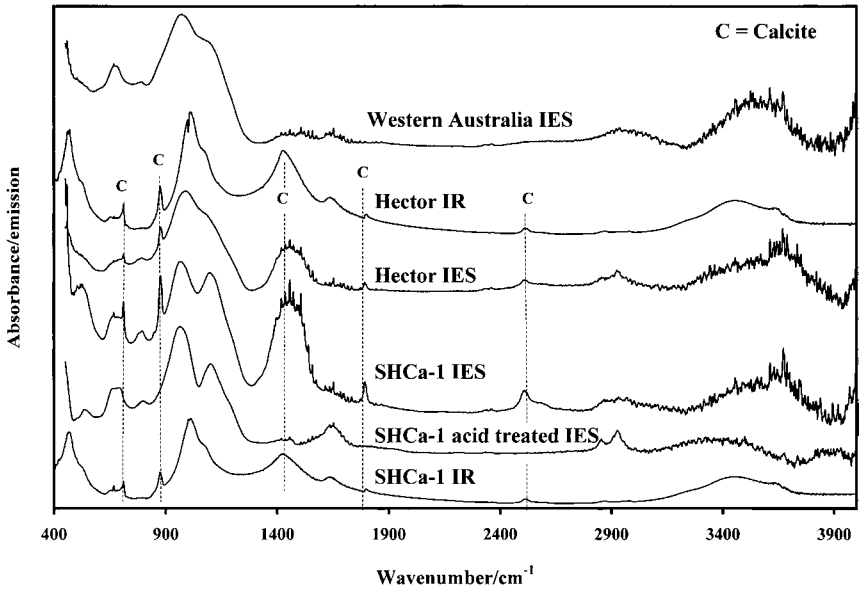

Fig. 2. Comparison of the infrared absorption and emission (200°C) spectra of selected hectorites.

Fig. 2 shows the comparison between the IR absorption spectra and the IES spectra. Generally speaking the bands in the IES spectra are somewhat broader and intensities may be different but the band positions are comparable but due to their broad nature may be shifted slightly in position. The spectra of the untreated samples clearly show the calcite carbonate stretching mode at 1475–1412 cm^{-1} and the bending mode around 875–870 cm^{-1}. The dolomite carbonate bands however are hardly distinguishable in especially the Western Australian sample. This may indicate that a minor amount of dolomite may already result in strong XRD reflections but is still undetectable by IR spectroscopic techniques. Other minor calcite bands can be recognised at 712, 1780–1800 and 2495–2530 cm^{-1}. The hectorite bands are summarised in Table 2.

The IES spectra in the region between 450 and 1300 cm^{-1} and between 3000 and 3800 cm^{-1} of the acetic acid treated hectorite SHCa-1 are shown in Fig. 3a and b. Band component analysis of the 200°C low frequency region reveal eight bands below 1300 cm^{-1} accompanied by still a minor band of the calcite around 1425 cm^{-1} and a bending vibration of water around 1650 cm^{-1} (Fig. 4a). Interesting is the presence of two OH deformation bands around 657 and 695 cm^{-1}, which agrees with in the literature indicated doublet in the OH stretching range (see e.g. [8,13]). Upon heating to 700°C significant differences become visible (Fig. 4b). The carbonate band around 1425 cm^{-1} has completely disappeared while the water band is actually no longer distinguishable from the background although band fitting indicate a very low intensity broad band. The SiO stretching bands show a broadening while the initially two sharp OH deformation bands with approximately equal intensity disappear and are replaced by one very small band around 690 cm^{-1} and a much stronger and broader band around 673 cm^{-1}. Also the MgO stretching band looses some intensity upon heating to 700°C. The 690 cm^{-1} band indicate the presence of a minor amount of OH left in the original crystal structure, whereas the formation of the 673 cm^{-1} band indicate a structural reorganisation in the octahedral layer of the hectorite.

The OH stretching region at 200°C clearly show the presence of the two M–OH stretching modes around 3647 and 3672 cm^{-1} although differential thermal analysis has shown that most water has already been lost around 165°C (Fig. 4c) and the two different water modes around 3300 and 3500 cm^{-1} [30]. Heating to 350°C results in complete removal of the two water

Table 2
Infrared absorption band positions of the standard hectorites in comparison with some literature values

SHCa-1 (this study)	SHCa-1 [10]	Hector (Ward's) (this study)	Hector [7,9]	Hector [13]	Hectorite (unknown origin) [8]	Assignment
3680	3678	3679	3675	3680	3670–3610 doublet?	OH stretch
3633		3636		3623		
3450	3420	3455	3427	3420	3450–3400	H_2O OH stretch
3249		3244		3225		H_2O OH stretch
1798	1795	1797				Calcite
1635	1625	1636	1626	1630	1650–1630	H_2O deformation
1422	1425	1425	1432	1430	1430	Calcite CO_3 stretch
1065	1078	1064	1070–1100	1078	1075–1073	SiO stretch
1010	1012	1008	1012–1015	1012	1011–1005	SiO stretch
875	875	874	874	877	873–853	Calcite CO_3 bend
798	800	798			820–780	Silica
	780			796		Silica
712	712	712			712–696	Calcite
702		703	701–703	696		Quartz
667	660	668		660		OH deformation
654		653	654–657		655	OH deformation
523	530	524	522	526	533–530	MgO stretch
468	470	469	467–469	467	470–465	SiO deformation
459		460		449		
424		428		427		
	315					Calcite

OH stretching bands but the hydroxyl bands are still clearly visible. Further heating to 750°C causes a decrease in the intensity of the M–OH stretching bands but they remain visible, which agrees well with the thermal analysis data reported by van Olphen and Fripiat [30], who indicated completion of the dehydroxylation by endotherms around 795°C with a shoulder around 725°C in the DTA pattern. Although the spectrum is quite noisy a sharp band can be distinguished in all spectra between 250°C and 750°C around 3741 cm^{-1}, which can be attributed to silanol groups. This band is also regularly observed in the spectra of other clay minerals around 3745 cm^{-1} [19,29,33–35]. In an earlier paper on the dehydroxylation of beidellite we have shown that these silanol groups can play an important role in the removal of water molecules formed by the recombination of two Mg–OH to a new Mg–O-type bond plus in the end an H_2O molecule [29].

The IES of the hectorite from Hector, CA, show not only the hectorite bands but also clearly recognisable calcite bands (Fig. 5). Except for the calcite bands at 712, 876 and 1457 cm^{-1} the band component analysis at 200°C for the low frequency region is comparable to the hectorite SHCa-1 discussed above (Fig. 6a). However, the bands are generally broader and more overlapping resulting in only one broad complex around 1050 cm^{-1} whereas for SHCa-1 still two complex bands around 950 and 1100 cm^{-1} can be distinguished. Heating to 700°C shows a minor difference with the hectorite SHCa-1 where a small band remained visible around 690 cm^{-1} together with a new band around 673 cm^{-1}. In this sample from Hector only one broad band is observed at 700°C around 690 cm^{-1} indicating a more complete rearrangement of the OH groups in the hectorite octahedral layer structure (Fig. 6b). This is also reflected in the OH stretching region where the M–OH bands are almost completely disappeared at 700°C. Like for the hectorite SHCa-1 the silanol band remains visible over the whole temperature range. The IES spectra of the hectorite from Western Australia (Fig. 7) are very similar to the spectra of the hectorite from Hector, CA. As in the infrared absorption spectrum of this hectorite

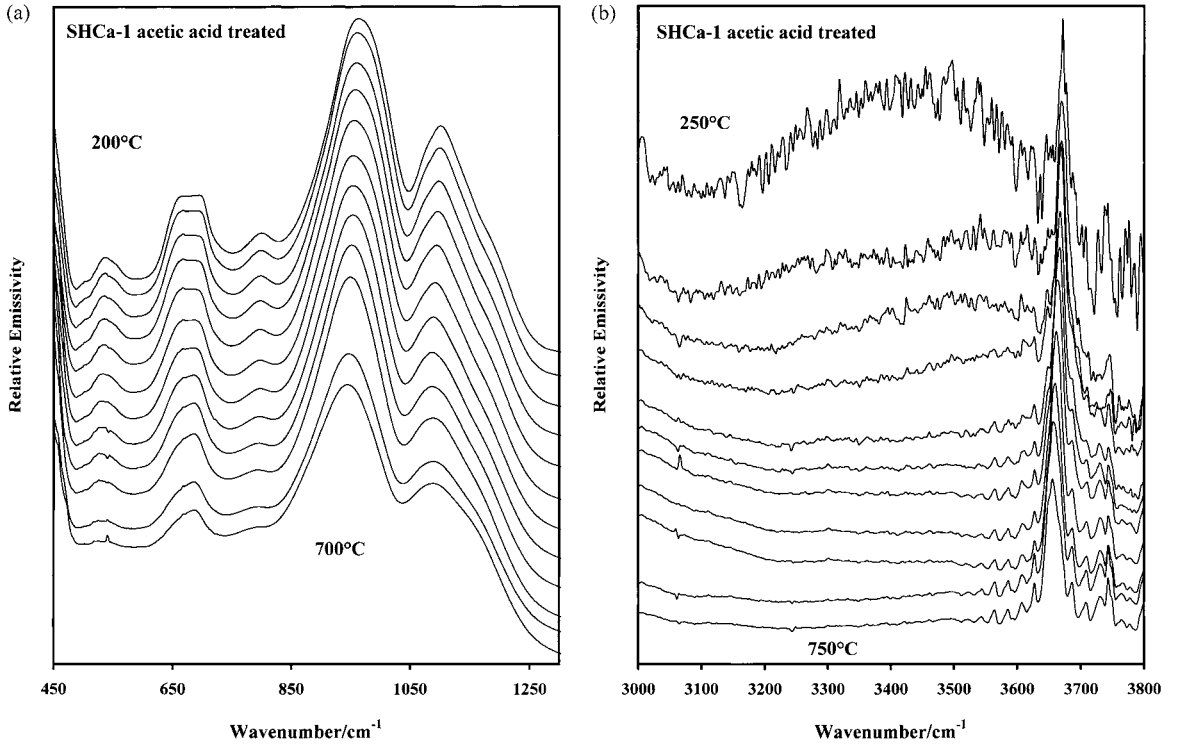

Fig. 3. IES of acetic acid treated hectorite SHCa-1 in the 450–1300 cm^{-1} region between 200°C and 700°C at 50°C (a), and in the hydroxyl stretching region between 200°C and 750°C at 50°C interval (b).

discussed above the dolomite is hardly visible. Only a very minor band can be observed near 650 cm^{-1} and a low intensity broad band around 1450 cm^{-1}.

4. Dehydroxylation model

Based on the changes in the IES of the hectorites in combination with the known thermogravimetric data [30] a model for the dehydroxylation can be given. Generally, the thermal decomposition sequence is comparable to that of talc, except that the interlayer water which is not present in talc is progressively lost and the dehydroxylation temperature is lowered by approximately 200°C due to the presence of Li and the interlayer cations in the hectorite structure [36]. Heating to 200°C for the first time IES results in a partial dehydration as evidenced by the water OH stretching bands in the 3000–3500 cm^{-1} region. This is in contrast with the thermogravimetric work which indicated that dehydration is completed for the SHCa-1 hectorite around 165°C [30,37]. The difference can be explained by the relatively rapid heating to 200°C in the infrared spectrometer giving the sample not enough time to loose all its adsorbed and interlayer water. Further heating quickly results in the removal of the remaining water.

The dehydroxylation starts around 250°C as evidenced by the decreasing intensity of both the Mg–OH stretching and bending modes. At 750°C still some intensity remains in the Mg–OH stretching modes indicating that the dehydroxylation is not yet complete, which is in accordance with the thermogravimetric data. The changes in the Mg–OH bending modes around 650–700 cm^{-1} however indicate that some structural reorganisation is taking place. Because the dehydroxylation is not complete at 750°C no new bands indicating the formation of new Mg–O–Mg, Mg–O–Li or Mg–O–Si bonds can be observed. An important observation is that above 250°C, when the dehydroxylation starts, a silanol band becomes visible. It is proposed that the reason for the

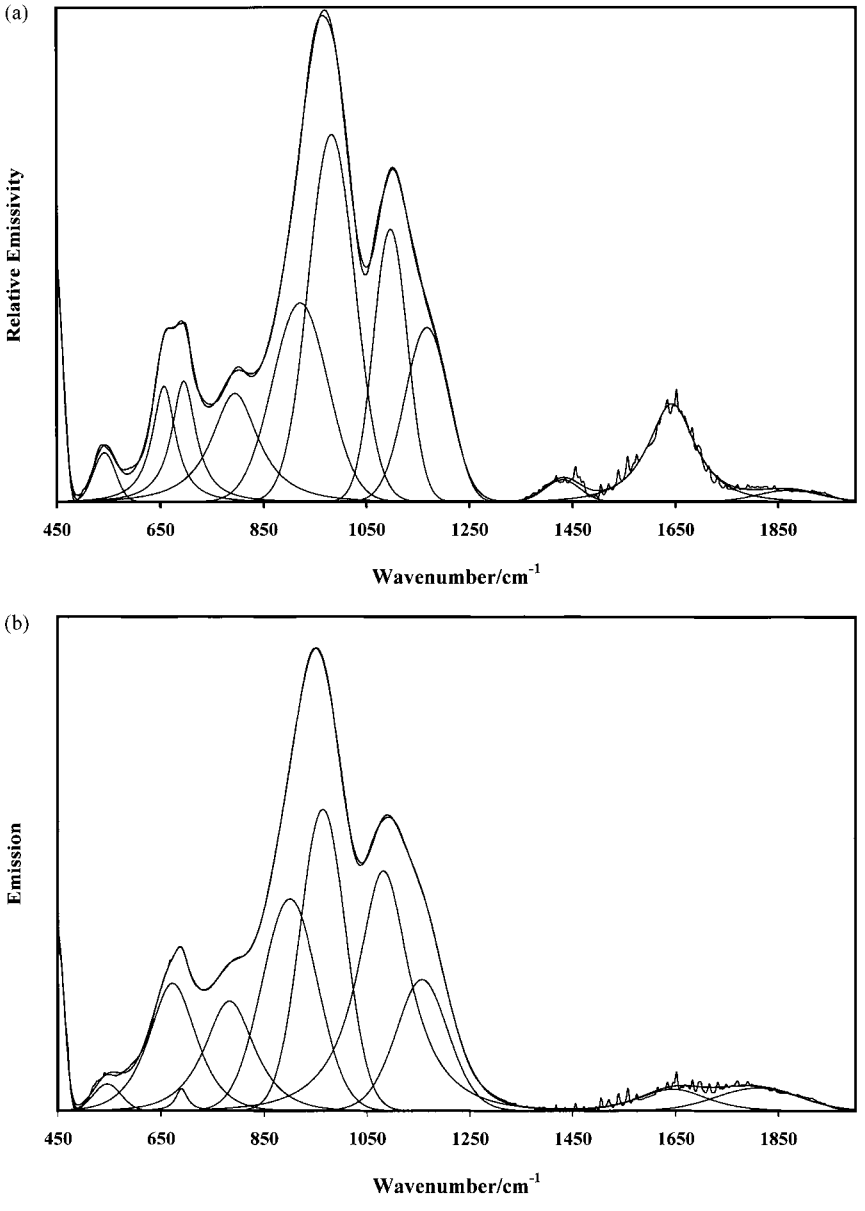

Fig. 4. Band component analysis of the low frequency region of the acid treated SHCa-1 infrared emission spectra at 200°C (a), at 700°C (b), and of the hydroxyl-stretching region at 200°C (c).

appearance of silanol bands is that the siloxane layer offers a mechanism for the dehydroxylation of the hectorite i.e. the hydroxyls are transferred upon thermal treatment to the Si and are then lost.

Pampuch suggested that dehydroxylation requires proton delocalisation at certain hydroxyl sites followed by migration to other hydroxyl sites where water molecules can be formed [38]. More or less similarly, Ball and Taylor have suggested that the dehydroxylation of brucite ($Mg(OH)_2$) is due to diffusional proton hopping counterbalanced by cation diffusion, leading to the formation of water molecules at

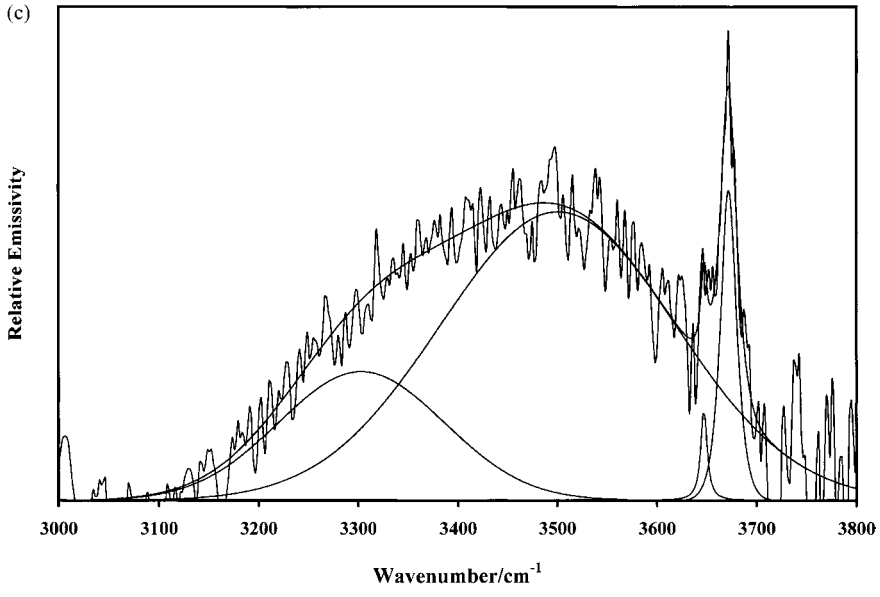

Fig. 4. (*Continued*).

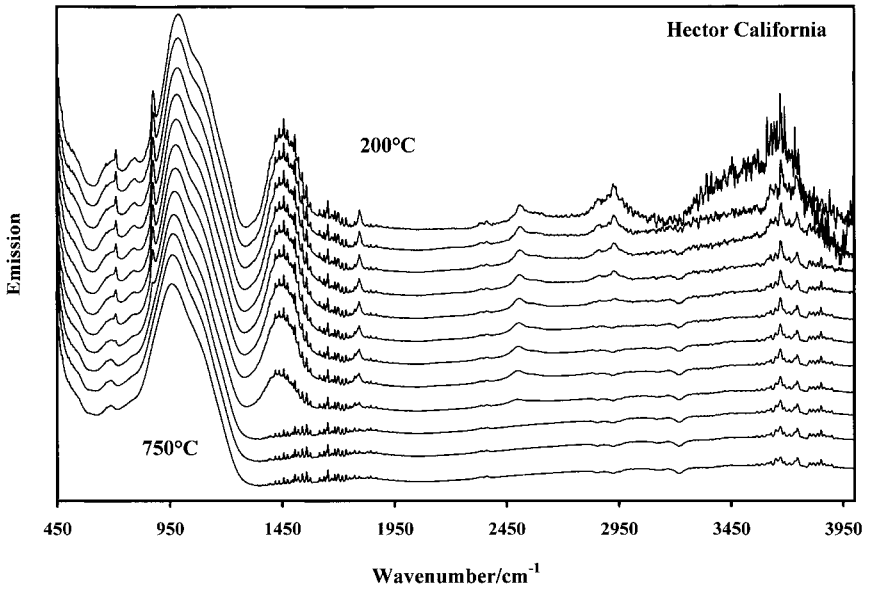

Fig. 5. IES of Ward's hectorite from Hector, CA between 200°C and 750°C at 50°C interval.

the outer surface of pores [39]. A similar process is very well possible for hectorite in which the octahedral layer is comparable to the brucite layer. Heller-Kallai and Rozenson [40] and Ogloza and Malhotra [41] indicated that in natural montmorillonites the dehydroxylation proceeds by protonation of hydroxyl groups adjacent to the site of negative charge starting from the surface. In the case of hectorite this would be near the Li-substituted octahedral sites resulting in the liberation of the Li followed by the possible diffusion

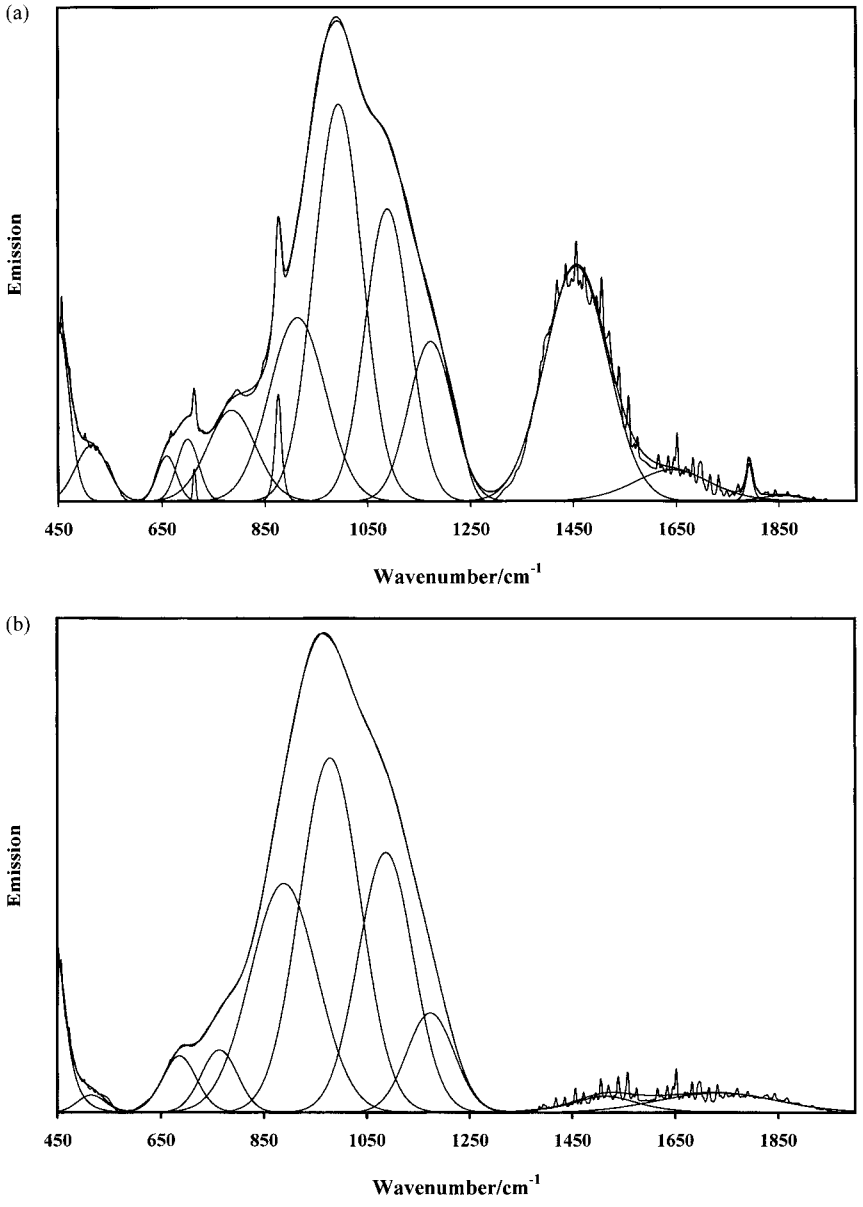

Fig. 6. Band component analysis of the low frequency region of the Ward's hectorite IES at 200°C (a), and at 700°C (b).

of Li through the clay structure. MacKenzie and Meinhold [42] observed the disruption of the hectorite structure above 600–650°C resulting in the formation of $MgSiO_3$ pyroxene-like units plus amorphous silica with distortion of the octahedral Mg sites. This would well explain the formation of the new band around 690 cm^{-1} as enstatite shows a similar band around 693–695 cm^{-1} [8] and the broadening of the bands in the low frequency region as the dehydroxylation proceeds.

The IES do not give any evidence of what happens to the lithium and other interlayer alkalies. MacKenzie and Meinhold [42] indicated that their NMR results for synthetic hectorite were not inconsistent with its

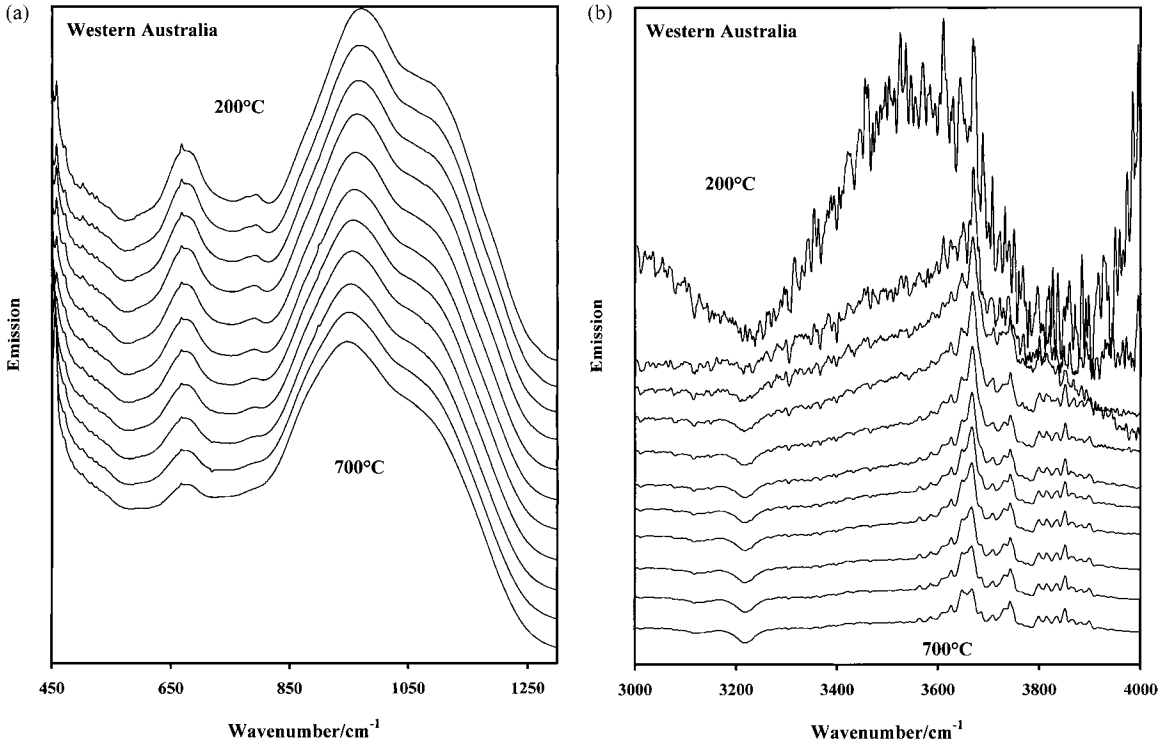

Fig. 7. IES of hectorite from Western Australia in the 450–1300 cm^{-1} region between 200°C and 700°C at 50°C (a), and in the hydroxyl stretching region (b), between 200°C and 700°C at 50°C.

incorporation in the siliceous phase. Mandair et al. [43] observed the irreversible breakdown to polymorphs of enstatite around 800°C and around 1300°C the enstatite polymorphs are accompanied by a glassy phase.

Acknowledgements

The financial and infra-structural support of the Queensland University of Technology, Centre for Instrumental and Developmental Chemistry is gratefully acknowledged. One of the authors (JTK) wishes to express his gratitude for the Postdoctoral Fellowship offered to him by the Queensland University of Technology.

References

[1] N. Güven, in: S.W. Bailey (Ed.), Hydrous Phyllosilicates (exclusive of micas), Reviews in Mineralogy 19 (1988) 497.
[2] W.A. Deer, R.A. Howie, J. Zussman, An Introduction to the Rock-Forming Minerals, reprinted 2nd ed., Addison Wesley, Harlow, 1996, 696 pp.
[3] J.T. Kloprogge, J. Porous Mater. 5 (1998) 5.
[4] A.C.D. Newman, Chemistry of Clays and Clay Minerals, Min. Soc. Monograph, vol. 6, London, 1987, 480 pp.
[5] J. Chaussidon, Clays Clay Miner. 18 (1970) 139.
[6] V.C. Farmer (Ed.), The Infrared Spectra of Minerals, Min. Soc. Monograph vol. 4, London, 1974, p. 331.
[7] P. Komadel, J. Madejova, M. Janek, W.P. Gates, R.J. Kirckpatrick, J.W. Stucki, Clays Clay Miner. 44 (1996) 228.
[8] J.A. Gadsden, Infrared Spectra of Minerals and Related Inorganic Compounds, Butterworth, London, 1975, 277 pp.
[9] J. Madejova, J. Bujdak, M. Janek, P. Komadel, Spectrochim. Acta A 54 (1998) 1397.
[10] V.C. Farmer, in: H. van Olphen, J.J. Fripiat (Eds.), Datahandbook for Clay Minerals and other Non-metallic Materials, Pergamon Press, Oxford, 1979, p. 285.
[11] K. Torii, T. Iwasaki, Clay Sci. 7 (1987) 1.
[12] R. Calvet, R. Prost, Clays Clay Miner. 19 (1971) 175.
[13] H.W. van der Marel, H. Beutelspacher, Atlas of Infrared Spectroscopy of Clay Minerals and their Admixtures, Elsevier, Amsterdam, 1976, 396 pp.
[14] J.T. Kloprogge, J.B.H. Jansen, J.W. Geus, Clays Clay Miner. 38 (1990) 409.

[15] J.T. Kloprogge, L. Hickey, R.L. Frost, Infrared study of some synthetic saponites: effect of NH_4/Al and H_2O/(Si(+(Al) ratios during the crystallisation, J. Mater. Sci. Lett. 18 (1999) 1401.
[16] S. Shimoda, Clay Miner. 9 (1971) 185.
[17] A.M. Vassallo, P.A. Cole-Clarke, L.S.K. Pang, A. Palmisano, J. Appl. Spectrosc. 46 (1992) 73.
[18] R.L. Frost, K. Finnie, B. Collins, A.M. Vassallo, in: R.W. Fitzpatrick, G.J. Churchman, T. Eggleton (Eds.), Proceedings of the 10th International Clay Conference, Adelaide, Australia, CSIRO Publications, Melbourne, July 1995, p. 219.
[19] R.L. Frost, A.M. Vassallo, Clays Clay Miner. 44 (1996) 635.
[20] J.T. Kloprogge, R.L. Frost, Klei, Glas and Keramiek 19 (1998) 11.
[21] J.T. Kloprogge, R.L. Frost, Thermochim. Acta 320 (1998) 245.
[22] J.T. Kloprogge, R.L. Frost, Infrared emission spectroscopic study of the dehydroxylation of synthetic Mg/Al and Mg/Zn/Al-hydrotalcite, Phys. Chem. Chem. Phys. 1 (1999) 1641.
[23] R.L. Frost, J.T. Kloprogge, S.C. Russell, J.L. Szetu, The vibrational spectroscopy and dehydroxylation of aluminium (oxo)hydroxides: gibbsite, Appl. Spectrosc. 53 (1999) 423.
[24] R.L. Frost, J.T. Kloprogge, J.L. Szetu, The dehydroxylation of aluminium (oxo)hydroxides using infrared emission spectroscopy: Part II Boehmite, Appl. Spectrosc. 53 (1999) 572.
[25] R.L. Frost, J.T. Kloprogge, J.L. Szetu, The dehydroxylation of aluminium (oxo)hydroxides using infrared emission spectroscopy, Part 3 diaspore. Appl. Spectrosc. 53 (1999) 829.
[26] R.L. Frost, J.T. Kloprogge, Infrared emission spectroscopic study of brucite, Spectrochim. Acta 55 (1999) 2195.
[27] J.T. Kloprogge, R.L. Frost, Neues Jahrb. Miner., Monatshefte, 1999, p. 62.
[28] J.T. Kloprogge, R. Fry, R.L. Frost, An infrared emission spectroscopic study of the thermal transformation mechanisms in $A1_{13}$-pillared clay catalysts with and without tetrahedral substitutions, J. Catal. 184 (1999) 157.
[29] J.T. Kloprogge, S. Komarneni, K. Yanagisawa, R. Fry, R.L. Frost, Infrared emission spectroscopic study of the dehydroxylation via surface silanol groups of synthetic and natural beidellite, J. Coll. Interf. Sci. 212 (1999) 562.
[30] H. van Olphen, J.J. Fripiat, Datahandbook for Clay Minerals and other Non-metallic Materials, Pergamon Press, Oxford, 1979, 346 pp.
[31] P. Komadel, M. Janek, J. Madejova, A. Weekes, C. Breen, J. Chem. Soc., Faraday Trans. 93 (1997) 4207.
[32] D.B. Levy, C. Amrhein, M.A. Anderson, A.M. Daoud, Soil. Sci. Soc. Am. J. 59 (1995) 1258.
[33] J.L. Ahlrichs, C. Serna, J.M. Serratosa, Clays Clay Miner. 23 (1975) 119.
[34] C. Serna, G.E. VanScoyoc, J.L. Ahlrichs, Am. Miner. 62 (1977) 784.
[35] R.J.M.J. Vogels, Non-hydrothermal synthesised trioctahedral smectites, Ph.D. Thesis, University of Utrecht, The Netherlands, 1996, pp. 31–86.
[36] J.M. Green, K.J.D. MacKenzie, J.H. Sharp, Clays Clay Miner. 18 (1970) 339.
[37] C.M. Earnest, Thermochim. Acta 63 (1983) 291.
[38] R. Pampuch, Bull. Groupe Fr. Argiles 23 (1971) 107.
[39] M.C. Ball, H.F.W. Taylor, Miner. Mag. 32 (1961) 754.
[40] L. Heller-Kallai, I. Rozenson, Clays Clay Miner. 28 (1980) 355.
[41] A.A. Ogloza, V.M. Malhotra, Phys. Chem. Miner. 16 (1989) 378.
[42] K.J.D. MacKenzie, R.H. Meinhold, Thermochim. Acta 232 (1994) 85.
[43] A.P.S. Mandair, P.J. Michael, W.R. McWhinnie, Polyhedron 9 (1990) 517.